The Canadian Mineralogist
Vol. 60, pp. 369-382 (2022)
DOI: 10.3749/canmin.2000122

SHAKHDARAITE-(Y), $ScYNb_2O_8$, FROM THE LESKHOZOVSKAYA GRANITIC PEGMATITE, THE VALLEY OF THE SHAKHDARA RIVER, SOUTHWESTERN PAMIR, GORNO-BADAKHSHANSKII AUTONOMOUS REGION, TAJIKISTAN: NEW MINERAL DESCRIPTION AND CRYSTAL STRUCTURE

LEONID A. PAUTOV

A.E. Fersman Mineralogical Museum, Russian Academy of Sciences, Leninskiy Prospekt 18-2, Moscow 119071, Russia
Federal State Budgetary Institute of Science, South Urals Research Center of Mineralogy and Geoecology, Urals Branch, Russian Academy of Sciences; SU FRC MG UB RAS, Miass, Chelyabinsk District, 456317, Russia

MIRAK A. MIRAKOV

Institute of Geology, Earthquake Engineering and Seismology, National Academy of Sciences of Tajikistan, Aini avenue, 267, Dushanbe, 734063, Tajikistan

ELENA SOKOLOVA[§], MAXWELL C. DAY, AND FRANK C. HAWTHORNE

Department of Earth Sciences, University of Manitoba, 125 Dysart Road, Winnipeg, Manitoba R3T 2N2, Canada

MANUCHEKHR A. SCHODIBEKOV

Institute of Geology, Earthquake Engineering and Seismology, National Academy of Sciences of Tajikistan, Aini avenue, 267, Dushanbe, 734063, Tajikistan

VLADIMIR YU. KARPENKO

A.E. Fersman Mineralogical Museum, Russian Academy of Sciences, Leninskiy Prospekt 18-2, Moscow 119071, Russia

SAIMUDASIR MAKHMADSHARIF AND ABDULKHAK R. FAIZIEV

Institute of Geology, Earthquake Engineering and Seismology, National Academy of Sciences of Tajikistan, Aini avenue, 267, Dushanbe, 734063, Tajikistan

ABSTRACT

Shakhdaraite-(Y), ideally $ScYNb_2O_8$, is a new mineral from the Leskhozovskaya miarolitic granitic pegmatite at the Shakhdara River, southwestern Pamir (Tajikistan). Shakhdaraite-(Y) occurs mainly as grains from 10 to 150 μm in size in a near-miarolitic pegmatite complex in association with quartz, albite, pyrochlore-microlite, fersmite, and an unnamed Sc-Nb oxide; only one large, single, well-shaped crystal 200 μm long was found in a small cavity with quartz, albite, bertrandite, pyrochlore, and jarosite. Shakhdaraite-(Y) is black to dark-brown, streak is brown. Luster is vitreous semi-metallic. It is brittle with conchoidal fracture. Mohs hardness is 5. $VHN_{100} = 436$ kg/mm^2. $D_{calc.} = 5.602$ g/cm^3. In reflected light, it is light gray and its reflective capacity is moderate to low. Anisotropy is distinct, without color effects. Pleochroism was not observed. Internal reflections are red-brown. Reflectance values were measured in air with SiC as reference material [λ(nm), R_{max}, R_{min}]: 470, 14.6, 13.9; 546, 14.0, 13.4; 589, 13.9, 13.3; 650, 13.8, 13.1. Electron probe microanalysis (WDS mode, 7 points) gives (wt.%): Nb_2O_5 50.70; Ta_2O_5 4.52; TiO_2 0.08; WO_3 0.79; SnO_2 1.54; CaO 1.01; Sc_2O_3 11.35; MnO 1.38; FeO 0.01; Y_2O_3 12.00; Ce_2O_3 0.21; Pr_2O_3 0.04; Nd_2O_3 0.27; Sm_2O_3 0.32; Eu_2O_3 0.07; Gd_2O_3 0.86; Tb_2O_3 0.22; Dy_2O_3 2.07; Ho_2O_3 0.29; Er_2O_3 1.33; Tm_2O_3 0.35; Yb_2O_3 2.80; Lu_2O_3 0.32; PbO 0.24; ThO_2 1.90; UO_2 3.30, total 97.97. The empirical formula of shakhdaraite-(Y) based on O = 8 *apfu* (atoms per formula unit) is $(Nb_{1.91}Sc_{0.83}Y_{0.53}Ta_{0.10}Mn_{0.10}Ca_{0.09}\ Yb_{0.07}U^{4+}_{0.06}Dy_{0.06}Sn_{0.05}Th_{0.04}Er_{0.03}Gd_{0.02}W^{6+}_{0.02}Pb_{0.01}Ce_{0.01}Nd_{0.01}Sm_{0.01}Tb_{0.01}Ho_{0.01}Tm_{0.01}Lu_{0.01}Ti_{0.01})_{\Sigma 4.00}O_8$, $Z = 2$. The simplified formula is $Sc(Y,Yb)Nb_2O_8$,

§ *Corresponding author e-mail address*: Elena.sokolova@umanitoba.ca

where Yb is the dominant lanthanoid. Shakhdaraite-(Y) is monoclinic, space group $P2/c$, a 9.930(2), b 5.6625(11), c 5.2108(10) Å, β 92.38(3)°, V 292.7(5) Å^3, $Z = 2$. The crystal structure was solved by direct methods [$R_1 = 0.0269$, 878 unique reflections ($F > 4\sigma F$)]. There are three cation M sites: $^{[6]}M(1) = Nb_2$ *apfu*, $^{[6]}M(2) = Sc$ *apfu*, and $^{[8]}M(3) = Y$ *apfu*, ideally $M = ScYNb_2$ *apfu*. The $M(1)$ and $M(2)$ octahedra each form a brookite chain along **c**. The Y-dominant $^{[8]}M(3A)$ polyhedra form a brookite-like kinked chain, and each $M(3A)$ polyhedron of one brookite-like chain shares two edges with the two $M(3A)$ polyhedra from the adjacent brookite-like chain, thus forming a $[Y_2O_8]^{10-}$ layer. In the structure of shakhdaraite-(Y), $M(1A)$ and $M(2)$ brookite chains and a layer of [8]-coordinated $M(3A)$ polyhedra alternate along **a**. Shakhdaraite-(Y) is isostructural with samarskite-(Y), ideally $YFe^{3+}Nb_2O_8$. Shakhdaraite-(Y) [Russian Cyrillic: шахдараит-(Y)] is named after its type locality: the valley of the Shakhdara River in the southwest of the Pamir Mountains.

Keywords: shakhdaraite-(Y), new mineral, crystal structure, electron probe microanalysis, rare-earth elements, niobium, granitic pegmatites, Shakhdara River, southwestern Pamir, Tajikistan.

Introduction

Shakhdaraite-(Y), ideally $ScYNb_2O_8$, is a new mineral from the Leskhozovskaya granitic pegmatite in the valley of the Shakhdara River, which is the left branch of the Gunt River, southwestern Pamir (Roshtkala district of Gorno-Badakhshanskii Autonomous Region, Tajikistan). There is only a small number of minerals with both Sc and Nb as species-forming elements, including the recently discovered niobohefteljernite, $ScNbO_4$, from Madagascar (Lykova *et al*. 2020) and various unnamed, poorly characterized phases, including "scandian ixiolite" (Nb,Ta,Ti,Sc,Fe,Mn)$_4O_8$, from Mozambique (von Knorring & Sahama 1969) and phases close in composition to $ScNbO_4$ from Southern Norway (Černý *et al*. 2000, Černý & Chapman 2001), Poland (Szełęg *et al*. 2010), and from the Czech Republic (Výravský *et al*. 2017). All these Sc-Nb minerals, including shakhdaraite-(Y), were discovered in granitic pegmatites. Shakhdaraite-(Y) is a Sc analogue of samarskite-(Y), ideally $YFe^{3+}Nb_2O_8$ (Britvin *et al*. 2019). Shakhdaraite-(Y) [Russian Cyrillic: шахдараит-(Y)] is named after its type locality: the valley of the Shakhdara River in the southwest of the Pamir Mountains. The new mineral and its name have been approved by the Commission on New Minerals, Nomenclature and Classification of the International Mineralogical Association (IMA 2020-024). The holotype specimen has been deposited in the collections of the Fersman Mineralogical Museum, Russian Academy of Sciences, Moscow, Russia; the registration number is 5569/1. Here we present the description and crystal structure of shakhdaraite-(Y), a new mineral.

Occurrence and Paragenesis

Shakhdaraite-(Y) was found in the Leskhozovskaya miarolitic granitic pegmatite (N 37° 11′ 43″ E 71° 52′ 04″) on the right slope of the valley of the Shakhdara River (middle course), which is a left tributary of the Gunt River, southwestern Pamir (Roshtkala district, Gorno-Badakhshanskii Autonomous Region, Tajikistan) (Fig. 1a). A.N. Labuntsov, a scientist from the Mineralogical Museum of the Academy of Sciences of the USSR, obtained the first data on the granitic pegmatites of southwestern Pamir as a member of the Tadjik-Pamir Expedition in 1928 (Labuntsov 1930). Since then, many pegmatites have been discovered in southwestern Pamir. The most well-known pegmatite veins occur in the Shakhdara River valley in the Shakhdarinskaya series of metamorphic rocks: Vezdarinskaya, Tusionskaya, Shakhdarinskaya, Badomdarinskaya, and Leskhozovskaya (Fig. 1b).

The age and origin of the more detailed stratigraphic subdivisions of the metamorphic rocks are not clear and still under investigation (Vinnichenko & Kukhtikov 1993). Most geologists consider the Shakhdarinskaya and Goranskaya series to be of Precambrian age (Budanova & Budanov 1983, Budanov 1993), although the radiometric age has been affected by processes associated with the India–Asia collision (Konovalenko 2009, Stübner *et al*. 2013, Stearns *et al*. 2015, Rutte *et al*. 2017). The granitic pegmatites in the Shakhdara River basin are associated with the large Pamiro-Shugnansky massif of high-alumina granite of Cenozoic age (Vladimirov *et al*. 2003, Vladimirov 2005, Konovalenko 2006). Melt inclusions in quartz indicate that the granites of the Pamiro-Shugnansky complex formed at temperatures from 740 to 660 °C and at a fluid pressure of 2.6–3.2 kbar (Chupin *et al*. 1988). The age of the pegmatite according to fission-track dating of apatite is estimated at 3.2–7.5 Ma, which is near to the time of the solidification of the Pamiro-Shugnansky complex granites (Konovalenko 2006).

The Leskhozovskaya pegmatite vein, where shakhdaraite-(Y) was discovered, occurs on the southwestern slope of the Shugnansky Range on the right bank of the Shakhdara River opposite the village of Shivoz, which is approximately 8.5 km upriver from the regional center of Roshtkala. The pegmatite vein is

exposed (Fig. 2a, b) about 100 m above the Khorog-Djavshangoz road and comprises a steeply dipping vein from 0.5 to 3.5 m wide that cuts the Precambrian garnet-biotite gneisses of the Shakhdarinskaya series. The pegmatite extends for 60–70 m (Konovalenko *et al*. 2001). The contacts of pegmatite with the country rock are sharp (Fig. 2c, d), and host-rock xenoliths are rare. The Leskhozovskaya pegmatite vein is a leucocratic aggregate of quartz, potassium feldspar, and sodic plagioclase with minor tourmaline and mica. There is a weak zonation in the pegmatite. There is an outer zone of fine-to-medium-granular "oligoclase" with biotite and schorl (Fig. 2d), and the core comprises a coarse-grained blocky pegmatitic feldspar with rare schorl and yellow-green tourmaline of the tsilaisite-elbaite series. Investigation of the melt inclusions in quartz from the pegmatite zone shows that the magmatic crystallization stage occurred from 550 to 600–650 °C at pressures from 2.2–2.8 to 3.8 kbar (Sazontova *et al*. 2003). In the pegmatite, there are miarolitic cavities from 0.5 m^3 to a fraction of a cm^3. There are large miarolitic cavities in wider parts of the pegmatite, with small cavities scattered throughout the pegmatite. The walls of the miarolitic cavities are encrusted with crystals of light-gray quartz, crystals of microcline and albite, rosettes of Li-bearing muscovite, and crystals of polychrome tourmaline. In the small cavities, light pink to colorless columnar to acicular elbaite is common. In the parts of the pegmatite with miarolitic cavities, there is extensive near-miarolitic texture, comprising light-gray quartz, lamellar and fine-grained albite, muscovite-lepidolite, and yellow-brown to yellow-green fluor-elbaite, the latter often growing on crystals of an earlier schorl. Boron-bearing fluids played a major role in the development of the pegmatite (Astrelina *et al*. 2011). The homogenization temperature of fluid inclusions in quartz from the Leskhozovskaya miarolitic pegmatite vein is 240–245 °C, and the boric acid concentration is 166–188 g/kg (Peretyazhko *et al*. 2000). In quartz and tourmaline in this particular pegmatite, sassolite was found for the first time as a constituent of fluid inclusions (Peretyazhko *et al*. 2000, Konovalenko *et al*. 2001, Smirnov *et al*. 2000, 2008).

The accessory minerals are zircon, xenotime-(Y), monazite-(Ce), almandine–spessartine, rutile, ilmenite, magnetite, uraninite, cassiterite, fersmite, native bismuth, fluorapatite, Sc-containing minerals of the wolframite group, pyrochlore-supergroup minerals, and bertrandite.

Shakhdaraite-(Y) is a very rare mineral in the pegmatite: only a few anhedral grains from 10 to 150 μm and one free-growing crystal 200 μm long were found in a near-miarolitic aggregate of albite and quartz, sometimes as intergrowths with pyrochlore-microlite (Fig. 3), fersmite, and an unknown Sc-Nb oxide. This crystal of shakhdaraite-(Y) was found in a small miarolitic cavity (1.5 cm across) in association with bertrandite, pyrochlore, albite, quartz, and jarosite (Fig. 4).

The chemical composition, reflectance spectra, microhardness, X-ray powder-diffraction pattern, and single-crystal X-ray data were obtained from the single crystal. The other remaining grains were used to obtain physical properties. All grains were checked using reflected-light microscopy, diffraction of back-scattered electrons (EBSD), and determination of chemical composition by electron probe microanalysis.

Physical and Optical Properties

Shakhdaraite-(Y) is dark-brown to black in color with a brown streak and vitreous semi-metallic luster. Cleavage was not observed; fracture is uneven to conchoidal. The hardness (VHN), obtained by microindentation tests with a PMT-3 instrument calibrated with NaCl, is 436 kg/mm^2 at 100 g load, and corresponds to a Mohs hardness of 5. Density (meas.) is higher than 4.24 g/cm^3 (grains sink in Clerici liquid). Other methods were not used due to the paucity of pure material. The calculated density, using the empirical formula, is 5.602 g/cm^3. The mineral does not luminesce either in short- (254 nm) or long-wave (315 nm) UV light. The mineral is non-magnetic. The only shakhdaraite-(Y) crystal found has dull faces unsuitable for measurement on a reflection goniometer (Fig. 4). The crystal is tabular. In reflected light, shakhdaraite-(Y) has a light-gray color with moderately low reflectance. Reflectance values were measured with a UMSP-50 Opton microspectrophotometer using the Opton SiC standard 474251 (with a spectral-slot width of 10 nm) and are given in Table 1. The mineral is characterized by normal dispersion. Anisotropy in air is distinct without color effects. Bireflectance was not observed. When observed in air, internal reflections are clearly seen and are brown in color.

Chemical Composition

The chemical composition of shakhdaraite-(Y) was measured by electron probe microanalysis with ED and WD spectrometers and by X-ray fluorescence. Preliminary analysis and estimation of grain homogeneity was done using a JSM-35FC scanning electron microscope equipped with a Si(Li)-detector and the ISIS analysis system of Oxford Instruments at the Institute of Geology, Earthquake Engineering, and Seismology (Dushanbe, Tajikistan) and using a JEOL JCXA-733 Superprobe electron microprobe equipped with a Si(Li)-detector and the INCA Energy 350

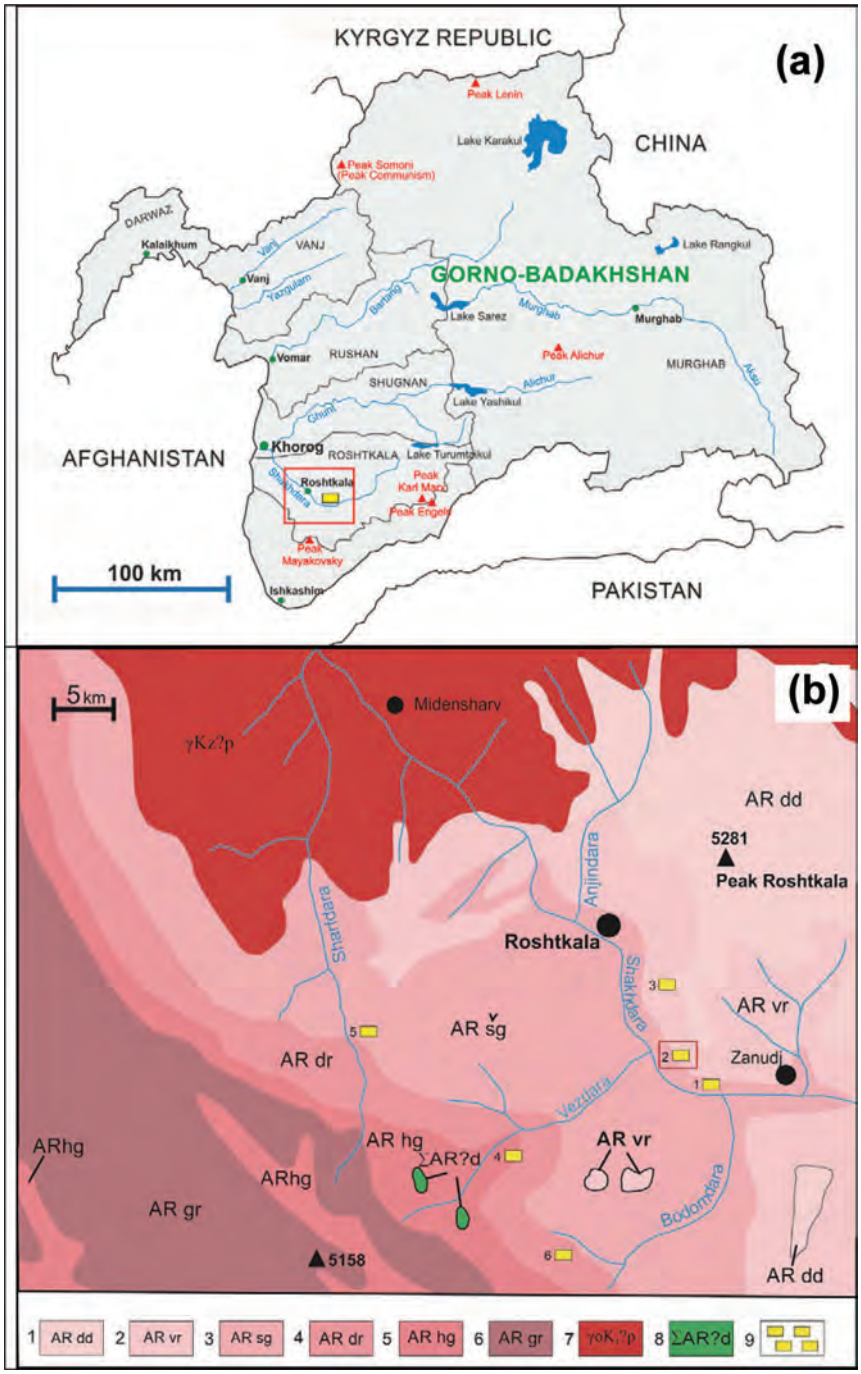

FIG. 1. Type locality of shakhdaraite-(Y): (a) geographic map of Tajikistan and (b) geological map. In (a), the yellow rectangle marks the shakhdaraite-(Y) type locality and the red frame shows the area of the detailed geological map of the Shakhdara River valley shown in (b). 5 – Archean(?) Shakhdarinskaya series, includes: 1 – Drumdarinskaya series: biotite, biotite-amphibole and biotite-garnet gneisses, migmatites, interlayered marbles, and kyanite-sillimanite gneisses; 2 – Wrangskaya series: biotite-amphibole and biotite-garnet gneisses, calcite and dolomite marbles; 3 – Shugnan series: biotite-garnet

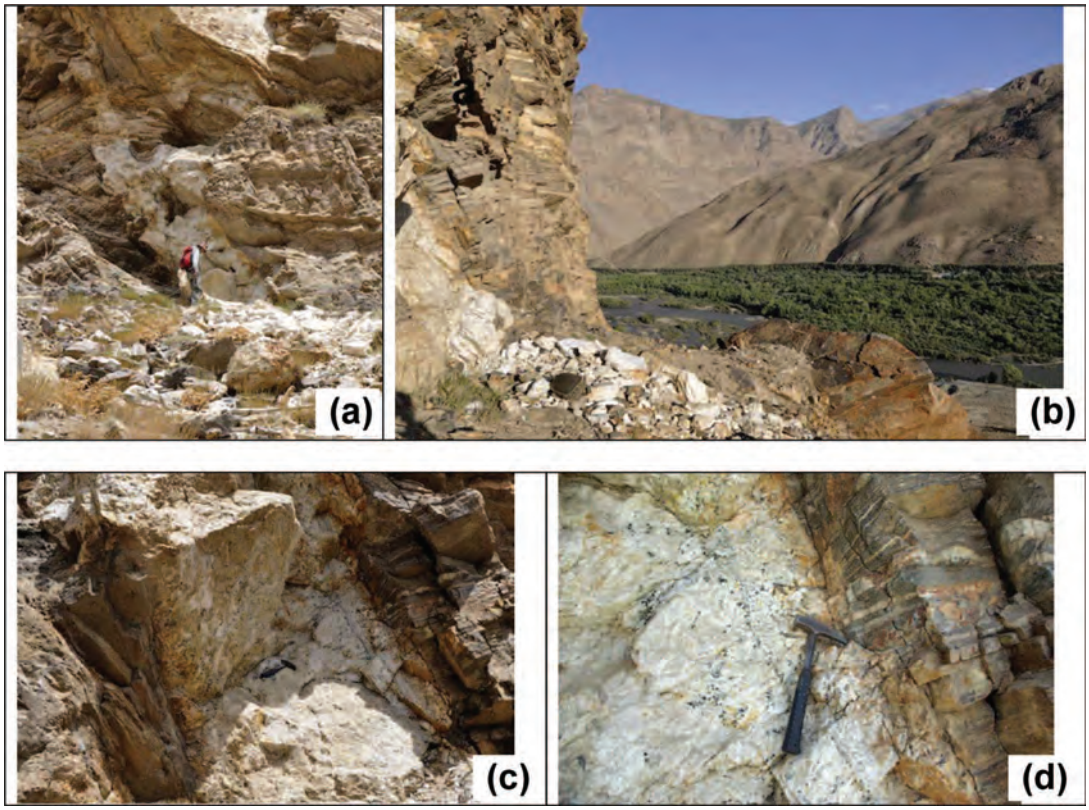

FIG. 2. The Leskhozovskaya pegmatite vein where shakhdaraite-(Y) was discovered: (a) a general view of the vein in gneisses of the Shakhdarinskaya series; (b) a view from the dumps of the vein in the direction of the Shakhdara River valley; (c) another view of the Leskhozovskaya pegmatite vein showing the sharp disconformity of the vein with the host gneisses; (d) a contact of the pegmatite with gneisses.

analysis system of Oxford Instruments in the laboratory of the Fersman Mineralogical Museum of the Russian Academy of Sciences (Moscow, Russia). The shakhdaraite-(Y) crystal was analyzed *in situ* in the cavity of the pegmatite sample using an EDAX EagleIII XRF with focused X-ray optics. The shakhdaraite-(Y) grains examined are characterized by minor variations in composition and the absence of zonation. Final analyses (number of analyses 7) were obtained using the JCXA-733 Superprobe in WDS mode at an acceleration voltage of 20 kV, beam current 30 nA and beam diameter 2–5 μm. Results are given in Table 2. Standards used were as follows [element (analytical line): standard]: Nb($L\alpha$): $Cs_2Nb_4O_{11}$; Mn($K\alpha$), Ta($M\alpha$): $MnTa_2O_6$; Ti($K\alpha$): Ilmenite USNM 96189; Sc($K\alpha$): Sc_2O_3; Fe($K\alpha$), W($M\beta$): $FeWO_4$; Ca($K\alpha$): $CaWO_4$; Th($M\alpha$): ThO_2; U($M\beta$): UO_2; Y($L\alpha$): Y_2O_3; La($L\alpha$): $LaPO_4$ USNM

←

FIG. 1. (continued) gneisses with interlayered biotite gneisses, marbles, migmatites, and amphibolite lenses; 4 – Darshayskaya series: biotite-garnet, amphibole-biotite-garnet, kyanite, sillimanite, two-pyroxene-garnet gneisses, migmatites, marbles; lenses of garnet granulites, meta-ultrabasites, eclogite-like rocks, and charnokites; 5 – Khorog series: garnet-amphibole-biotite gneisses and schists, amphibolites, interlayered garnet and two-pyroxene gneisses, lenses of meta-ultrabasites, eclogite-like rocks, and charnokites; 6 – Archean(?) Goranskaya series: biotite, amphibole-biotite, and sillimanite-biotite gneisses; quartzites, migmatites, interlayered granulites and magnesite marbles, carbonate-silicate rock, lenses of eclogite-like rocks, and amphibolites; 7 – lower-Cenozoic(?) Pamiro-Shugnan complex: biotite, muscovite, binary granites; 8 – Darshay complex: ultrabasites, gabbro, gabbro-norite; 9 – granite pegmatites: 1 – Pridorozhnyi, 2 – Leskhozovsky [shakhdaraite-(Y) type locality], 3 – Shakhdarinsky, 4 – Vezdarinsky, 5 – Tusionsky, 6 – Bodomdara.

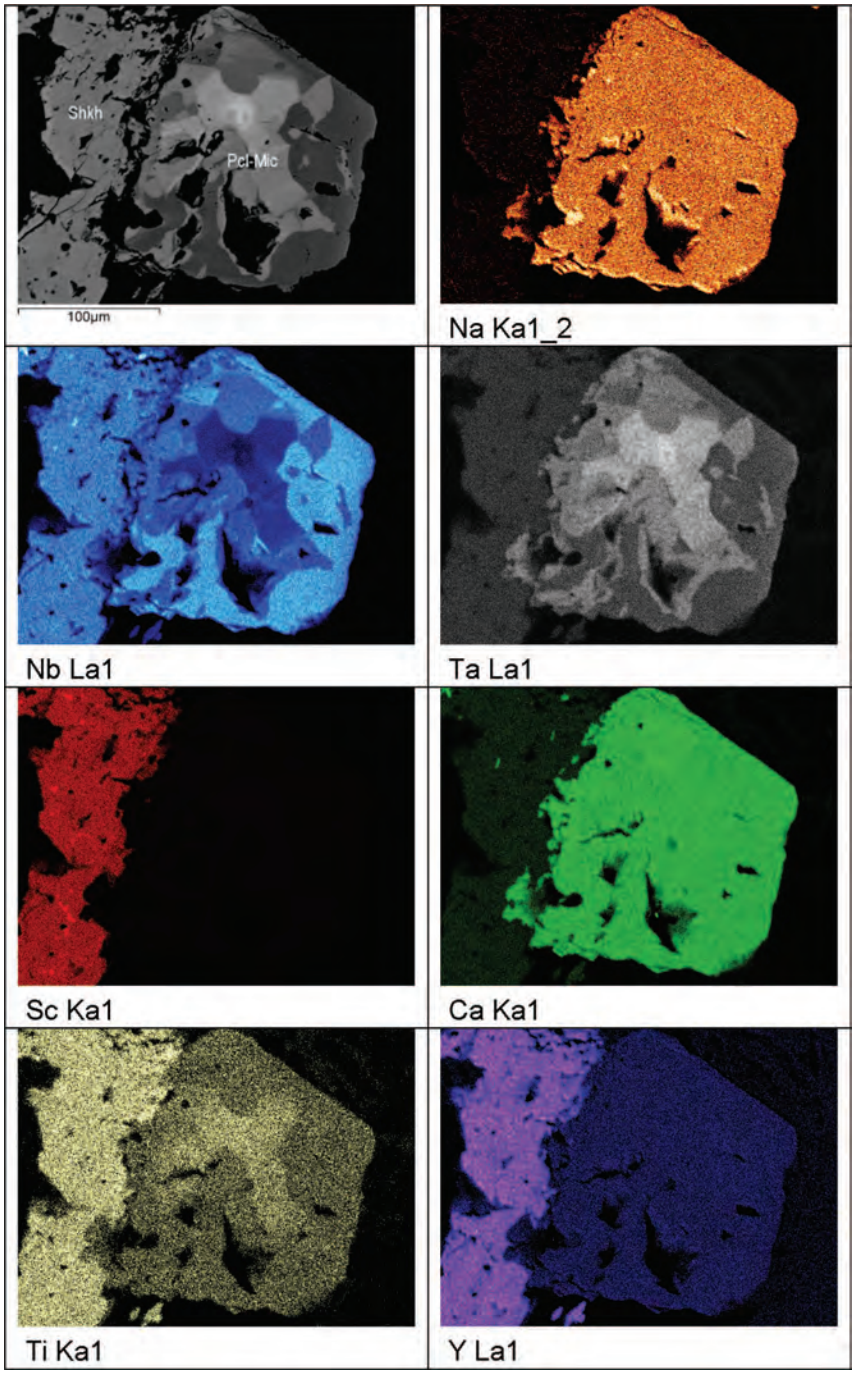

FIG. 3. Shakhdaraite-(Y) (Shkh) intergrowth with a sector-zoned crystal of pyrochlore-microlite (Pcl-Mic). Top left: BSE image. Others: X-ray distribution maps of the specified elements.

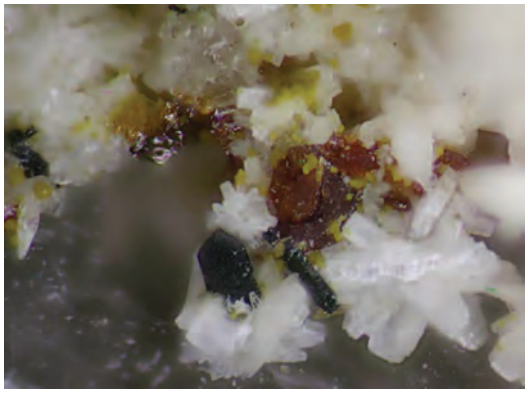

FIG. 4. A black crystal of shakhdaraite-(Y) with pyrochlore (red crystals), bertrandite (white crystals), and jarosite (yellow crystals); the gray field in the lower part of the image is quartz. Field of view is 2.5 mm.

168490; Ce($L\alpha$): $CePO_4$ USNM 168484; Pr($L\beta$): $PrPO_4$ USNM 168493; Sm($L\alpha$): $SmPO_4$ USNM 168494; Nd($L\alpha$): $NdPO_4$ USNM 168492; Dy($L\beta$): Dy_2O_3; Ho($L\beta$): Ho_2O_3; Er($L\beta$): Er_2O_3; Tb($L\alpha$): $TbPO_4$ USNM 168496; Yb($L\alpha$): $YbPO_4$ USNM 168498; Gd($L\alpha$): $GdPO_4$ USNM 168488; Tm($L\alpha$): $TmPO_4$ USNM 168497; Lu($L\alpha$): $LuPO_4$ USNM 168491; Eu($L\alpha$): $EuPO_4$ USNM 168487; Pb($L\alpha$): $PbTiO_3$. The spectral overlap on the analytical lines for Ta($M\alpha$), Y($L\alpha$), Er($L\beta$), Nd(La), and Eu($L\alpha$) was corrected. The data were reduced and corrected by the PAP method of Pouchou & Pichoir (1985). The empirical formula of shakhdaraite-(Y) based on 8 O *apfu* is $(Nb_{1.91}Sc_{0.83}Y_{0.53}Ta_{0.10}Mn_{0.10}Ca_{0.09}Yb_{0.07}U^{4+}_{0.06}Dy_{0.06}Sn_{0.05}Th_{0.04}Er_{0.03}Gd_{0.02}W^{6+}_{0.02}Pb_{0.01}Ce_{0.01}Nd_{0.01}Sm_{0.01}Tb_{0.01}Ho_{0.01}Tm_{0.01}Lu_{0.01}Ti_{0.01})_{\Sigma 4.00}O_8$. The simplified formula is $Sc(Y,Yb)Nb_2O_8$ ($Z = 2$), where Yb is the dominant lanthanoid. The ideal formula is $ScYNb_2O_8$, which requires Sc_2O_3 15.40, Y_2O_3 25.22, Nb_2O_5 59.38, total 100 wt.%.

TABLE 1. REFLECTANCE VALUES (%) OF SHAKHDARAITE-(Y)

R_{max}	R_{min}	λ (nm)	R_{max}	R_{min}	λ (nm)
15.6	14.8	400	14.0	13.3	560
15.4	14.6	420	13.9	13.3	580
15.2	14.3	440	13.9	13.3	589
14.7	14.0	460	13.8	13.2	600
14.6	13.9	470	13.8	13.1	620
14.4	13.8	480	13.8	13.1	640
14.3	13.6	500	13.8	13.1	650
14.1	13.5	520	13.7	13.0	660
14.0	13.4	540	13.7	13.0	680
14.0	13.4	546	13.7	13.0	700

TABLE 2. CHEMICAL COMPOSITION AND UNIT FORMULA* FOR SHAKHDARAITE-(Y)

Constituent	wt.%	Range		*apfu*
WO_3	0.79	0.24–1.22	W^{6+}	0.02
Ta_2O_5	4.52	4.26–5.63	Ta	0.10
Nb_2O_5	50.70	49.71–52.06	Nb	1.91
UO_2	3.30	3.23–3.42	U^{4+}	0.06
ThO_2	1.90	1.89–3.40	Th	0.04
SnO_2	1.54	1.14–1.74	Sn	0.05
TiO_2	0.08	0.07–0.28	Ti	0.01
La_2O_3	0.00	0.00–0.12	La	0
Ce_2O_3	0.21	0.05–0.34	Ce	0.01
Pr_2O_3	0.04	0.02–0.22	Pr	0
Nd_2O_3	0.27	0.26–0.44	Nd	0.01
Sm_2O_3	0.32	0.29–0.58	Sm	0.01
Eu_2O_3	0.07	0.05–0.24	Eu	00
Gd_2O_3	0.86	0.45–1.11	Gd	0.02
Tb_2O_3	0.22	0.14–0.31	Tb	0.01
Dy_2O_3	2.07	1.68–2.31	Dy	0.06
Ho_2O_3	0.29	0.19–0.71	Ho	0.01
Er_2O_3	1.33	1.13–1.61	Er	0.03
Tm_2O_3	0.35	0.12–0.35	Tm	0.01
Yb_2O_3	2.80	2.33–2.81	Yb	0.07
Lu_2O_3	0.32	0.19–0.32	Lu	0.01
Y_2O_3	12.00	11.29–12.15	Y	0.53
Sc_2O_3	11.35	11.27–11.48	Sc	0.83
PbO	0.24	0.17–0.86	Pb	0.01
FeO	0.01	0.01–0.11	Fe^{2+}	0
MnO	1.38	1.20–1.49	Mn	0.10
CaO	1.01	0.88–1.37	Ca	0.09
Total	97.97		Σcat	4.00

* Formula unit calculated on 8 O *apfu*.

X-RAY POWDER-DIFFRACTION DATA

X-ray powder-diffraction data for shakhdaraite-(Y) were collected with an RKU-86 camera (diameter 86 mm) using Fe$K\alpha$ radiation, a Mn-filter, and quartz as an internal standard (Table 3). Intensities of reflections were estimated by photometric measurement of optical density of a scanned film with Pspectr software. Unit-cell parameters refined from powder data are a = 9.92(1) Å, b = 5.666(5) Å, c = 5.207(3) Å, β = 92.33(7)°, V = 292.4(7) Å^3.

CRYSTAL STRUCTURE

Data collection and structure refinement

Single-crystal X-ray data were collected from a crystal of shakhdaraite-(Y) (0.04 × 0.03 × 0.02 mm)

TABLE 3. X-RAY POWDER-DIFFRACTION DATA* FOR SHAKHDARAITE-(Y)

I_{meas}	d_{meas} (Å)	I_{calc}	d_{calc} (Å)	*h k l*
3	9.8		9.921	1 0 0
35	3.72	26	3.731	2 1 0
8	3.60	5	3.612	1 1 $\bar{1}$
100	3.073	100	3.079	$\bar{2}$ 1 1
85	2.990	96	2.989	2 1 1
20	2.832	18	2.831	0 2 0
24	2.603	21	2.603	0 0 $\bar{2}$
33	2.484	19	2.487	0 $\bar{2}$ 1
			2.480	4 0 0
13	2.208	7	2.206	2 2 1
2	2.107	5	2.104	2 1 2
23	1.916	17	1.916	0 2 $\bar{2}$
21	1.867	17	1.866	4 2 0
17	1.831	13	1.834	4 0 $\bar{2}$
4	1.805	1	1.806	2 2 $\bar{2}$
18	1.767	18	1.769	2 2 2
			1.764	2 3 0
18	1.759	18	1.760	4 0 2
9	1.737	11	1.739	4 2 1
5	1.656	4	1.659	0 $\bar{1}$ 3
12	1.591	11	1.593	$\bar{2}$ 1 3
12	1.555	10	1.555	$\bar{2}$ 1 $\bar{3}$
			1.554	$\bar{3}$ 3 $\bar{1}$
14	1.538	11	1.539	$\bar{4}$ 2 2
			1.536	5 2 $\bar{1}$
			1.536	$\bar{5}$ $\bar{2}$ $\bar{1}$

* Fe$K\alpha$ radiation, Mn-filter, quartz was used as an internal standard.
Reflection intensities were estimated by means of photometric evaluation of optical density of a scanned film with Pspectr software.

TABLE 4. MISCELLANEOUS REFINEMENT DATA FOR SHAKHDARAITE-(Y)

a (Å)	9.930(2)
b	5.6625(11)
c	5.2108(10)
β (°)	92.38(3)
V (Å^3)	292.7(5)
Space group	*P2/c*
Z	2
Reflections ($I > 10\sigma I$)	5159
Absorption coefficient (mm^{-1})	18.84
F(000)	891.2
$D_{calc.}$ (g/cm^3)	5.602
Crystal size (mm)	0.040 × 0.030 × 0.020
Radiation/monochromator	Mo$K\alpha$/graphite
2θ-range for data collection (°)	62.40
*h**	$-14 \leq h \leq 14$
*k**	$-8 \leq k \leq 8$
*l**	$-7 \leq l \leq 7$
R(int)	0.0166
Reflections collected	3725
Independent reflections	948
$F_o > 4\sigma F$	878
Refinement method	Full-matrix least squares on F^2, fixed weights proportional to $1/\sigma F_o^2$
Final *R*(obs)	
$R_1(F_o > 4\sigma F)$	0.0269
R_1	0.0316
wR_2	0.0628
Goodness of fit on F^2	1.157
Highest peak, deepest hole (e Å^{-3})	1.14, –0.98

with a Bruker APEX II ULTRA three-circle diffractometer with a rotating-anode generator (Mo$K\alpha$), multilayer optics, and an APEX II 4K CCD detector. Unit-cell parameters from the single-crystal data were determined by least-squares refinement of 5159 reflections with $I > 10\sigma I$ and are given in Table 4, together with miscellaneous information on data collection and structure refinement. For shakhdaraite-(Y), the intensities of 3725 reflections were measured using 10 s per 0.5° frame. An absorption correction was done using the SADABS program (Sheldrick 2015). The crystal structure was solved by direct methods in space group *P*2/*c* and refined to $R_1 = 0.0269$ on the basis of 878 unique reflections ($F > 4\sigma F$). All calculations were done with the Bruker SHELXTL-2014/3 (version 3) system of programs (Sheldrick 2015). Scattering curves for neutral atoms were taken from the International Tables for Crystallography (Wilson 1992). Occupancies of the *M*(1A) and *M*(1B) sites were refined with the scattering curve of Nb, *M*(2) site: Sc, *M*(3A) and *M*(3B) sites: Y. The *M*(1A) and *M*(1B) sites are 0.32 Å apart and the *M*(3A) and *M*(3B) sites are 0.28 Å apart, hence these four sites can only be alternately occupied. Atom coordinates and anisotropic displacement parameters are listed in Table 5, selected interatomic distances are reported in Table 6, and refined site-scattering values and assigned site populations are given in Table 7. A CIF file and a list of structure factors may be obtained from The Depository of Unpublished Data on the MAC website[1].

Assignment of site populations

In the structure, there are three cation *M*(1–3) sites (Table 5). The [6]-coordinated *M*(1) site is split into

[1] Available from http://mineralogicalassociation.ca/, document "Shakhdaraite, CM60, 20-00122".

TABLE 5. ATOM COORDINATES AND ANISOTROPIC DISPLACEMENT PARAMETERS (Å^2) FOR SHAKHDARAITE-(Y)

Atom	*x*	*y*	*z*	U^{11}	U^{22}	U^{33}	U^{23}	U^{13}	U^{12}	U^{eq}
M(1A)	0.75537(18)	0.3147(4)	0.2262(8)	0.0147(3)	0.0139(5)	0.0118(7)	0.0017(4)	–0.0031(3)	–0.0001(2)	0.0136(4)
M(1B)	0.746(2)	0.291(4)	0.278(6)	0.030(5)	0.035(5)	0.013(5)	0.011(4)	–0.002(3)	–0.001(3)	0.026(3)
M(2)	0	0.81831(14)	¼	0.0168(4)	0.0202(4)	0.0164(4)	0	–0.0001(3)	0	0.0178(2)
M(3A)	½	0.7706(9)	¼	0.0128(5)	0.0151(10)	0.0097(6)	0	0.0007(3)	0	0.0126(5)
M(3B)	½	0.820(6)	¼	0.025(3)	0.026(7)	0.029(3)	0	0.0045(15)	0	0.026(3)
O1	0.6247(4)	1.0980(6)	0.0913(7)	0.0326(19)	0.0228(16)	0.0269(17)	–0.0006(13)	0.0025(13)	–0.0015(14)	0.0274(8)
O2	0.6381(4)	0.5794(7)	0.0123(9)	0.0269(19)	0.036(2)	0.055(3)	0.0210(19)	–0.0025(17)	0.0023(16)	0.0394(11)
O3	0.8621(4)	0.3885(6)	–0.0824(6)	0.0280(17)	0.0201(15)	0.0248(16)	0.0025(12)	–0.0016(12)	0.0024(13)	0.0244(8)
O4	0.8855(3)	0.1145(6)	0.4082(6)	0.0242(16)	0.0215(15)	0.0262(16)	–0.0039(12)	–0.0002(12)	–0.0006(12)	0.0240(8)

TABLE 6. INTERATOMIC DISTANCES (Å) FOR SHAKHDARAITE-(Y)

M(1A)–O(1)a	1.900(4)	M(2)–O(3)c,f	2.027(4) ×2
M(1A)–O(4)	1.937(4)	M(2)–O(1)c,e	2.108(3) ×2
M(1A)–O(3)	2.007(5)	M(2)–O(4)d,g	2.205(4) ×2
M(1A)–O(2)b	2.021(5)	<M(2)–O>	2.113
M(1A)–O(2)	2.176(5)		
M(1A)–O(3)b	2.204(4)	M(3A)–O(2)h	2.175(5) ×2
<M(1A)–O>	2.041	M(3A)–O(1)i,j	2.251(4) ×2
		M(3A)–O(1)h	2.395(5) ×2
M(1B)–O(4)	1.82(2)	M(3A)–O(2)k,b	2.742(6) ×2
M(1B)–O(2)b	1.81(3)	<M(3A)–O>	2.391
M(1B)–O(1)a	1.87(2)		
M(1B)–O(3)b	2.25(2)	M(3B)–O(1)i,j	2.174(8) ×2
M(1B)–O(3)	2.31(4)	M(3B)–O(1)h	2.19(2) ×2
M(1B)–O(2)	2.37(3)	M(3B)–O(2)h	2.33(2) ×2
<M(1B)–O>	2.07	<M(3B)–O>	2.23
M(1A)–M(1B)	0.32(3)	M(3A)– M(3B)	0.28(3)

Symmetry operators: a: x, y–1, z; b: x, –y+1, z+$^1/_2$; c: –x+1, –y+1, –z+1; d: –x+1, y+1, –z+$^1/_2$; e: x–1, –y+1, z–$^1/_2$; f: x–1, –y+1, z+$^1/_2$; g: x–1, y+1, z; h: –x+1, y, –z+$^1/_2$; i: –x+1, –y+2, –z; j: x, –y+2, z+$^1/_2$; k: –x+1, –y+1, –z.

two sites, *M*(1A) and *M*(1B), 0.32 Å apart (Table 6), and hence they can only be alternately occupied. The refined-scattering values for the *M*(1A) and *M*(1B) sites are 73.5 and 8.5 *epfu* (electrons per formula unit), respectively (Table 7). The mean distances for the *M*(1A) and *M*(1B) sites are 2.041 and 2.07 Å, respectively; subtraction of $r(^{[4]}O^{2-})$ = 1.38 Å (Shannon 1976) from each mean distance gives calculated aggregate cation radii of 0.661 and 0.69 Å, respectively. Hence we assign $(Nb_{1.76}Ta_{0.03}Ti_{0.01}\square_{0.20})$ *pfu* to the *M*(1A) site [calculated site-scattering of 74.57 *epfu*] and $(Nb_{0.15}Sn_{0.05}\square_{0.80})$ *pfu* to the *M*(1B) site [calculated site-scattering of 8.65 *epfu*] (Table 6), *i.e.*, all Sn is assigned to the *M*(1B) site (*cf.* $^{[6]}$Nb: $r = 0.64$ Å, $^{[6]}$Ta: $r = 0.64$ Å, $^{[6]}$Ti: $r = 0.605$ Å, $^{[6]}$Sn: $r = 0.69$ Å, Shannon 1976). The refined-scattering value for the [6]-coordinated *M*(2) site is 30.9 *epfu*, <*M*(2)–O> = 2.113 Å (Tables 4–6). We assign $(Sc_{0.83}Ta_{0.07}Mn_{0.04}U^{4+}{}_{0.03}W^{6+}{}_{0.02}Pb_{0.01})$ *apfu* to the *M*(2) site, with a calculated site-scattering of 28.60 *epfu*. For the *M*(2) site, *M*(2)–O distances vary from 2.027 to 2.205 Å, in accord with 450 Sc–O distances in 75 polyhedra (1.995–2.231 Å) reported by Gagné & Hawthorne (2020). The *M*(3) site splits into two sites, [8]-coordinated *M*(3A) and [6]-coordinated *M*(3B), separated by a short distance of 0.28 Å and hence they can only be alternately occupied. The refined-scattering values for the *M*(3A) and *M*(3b) sites are 38.6 and 9.5 *epfu*, respectively; <*M*(3A)–O> = 2.391 Å and <*M*(3B)–O> = 2.23 Å (Tables 5–7). We assign $(Y_{0.53}Ln_{0.25}\square_{0.22})$ *pfu* to the *M*(3A) site

TABLE 7. REFINED SITE-SCATTERING VALUES AND ASSIGNED SITE-POPULATIONS FOR SHAKHDARAITE-(Y)

Site	Refined site-scattering (*epfu*)	Assigned site population (*apfu*)	Calculated site-scattering (*epfu*)	<Ct–O>$_{obs}$* (Å)	Ideal composition (*apfu*)
$^{[6]}M$(1A)	73.5(1.9)	$Nb_{1.76}Ta_{0.03}Ti_{0.01}\square_{0.20}$	74.57	2.041	Nb_2
$^{[6]}M$(1B)	8.5(1.9)	$Nb_{0.15}Sn_{0.05}\square_{0.80}$	8.65	2.07	□
ΣM(1)	82.0	$Nb_{1.91}Sn_{0.05}Ta_{0.03}Ti_{0.01}$	83.22		Nb_2
$^{[6]}M$(2)	30.9(3)	$Sc_{0.83}Ta_{0.07}Mn_{0.04}U^{4+}{}_{0.03}W^{6+}{}_{0.02}Pb_{0.01}$	28.60	2.113	Sc
$^{[8]}M$(3A)	38.6(1.7)	$Y_{0.53}Ln_{0.25}\square_{0.22}$	37.37	2.391	Y
$^{[6]}M$(3B)**	9.5(1.7)	$Ca_{0.09}Mn_{0.06}Th_{0.04}U^{4+}{}_{0.03}\square_{0.78}$	9.66	2.23	□
ΣM(3)	48.1	$Y_{0.53}Ln_{0.25}Ca_{0.09}Mn_{0.06}Th_{0.04}U^{4+}{}_{0.03}$	47.03		Y

* Ct = cation;

** $Ln_{0.25}$ = ($Yb_{0.07}Dy_{0.06}Er_{0.03}Gd_{0.02}Ce_{0.01}Nd_{0.01}Sm_{0.01}Tb_{0.01}Ho_{0.01}Tm_{0.01}Lu_{0.01}$); corresponding f-curve of 66.8 el.

(calculated site-scattering of 37.37 *epfu*) and ($Ca_{0.09}Mn_{0.06}Th_{0.04}U^{4+}{}_{0.03}\square_{0.78}$) *pfu* to the *M*(3B) site (calculated site-scattering of 9.66 *epfu*) (Table 7). Assignment of Y and *Ln* (where Yb is the dominant *Ln*) to the *M*(3A) site is supported by the value of the mean bond-length: 2.391 Å (Table 6): $r(^{[8]}Y) = 1.019$ Å; $r(^{[8]}Yb^{3+}) = 0.985$ Å; $r(^{[4]}O^{2-}) = 1.38$ Å (Shannon 1976); $1.019 \times {}^{2}/_{3} + 0.985 \times {}^{1}/_{3} + 1.38 = 2.391$ Å.

Description of the crystal structure

In the structure, the Nb-dominant *M*(1A) site and the vacancy-dominant *M*(1B) site are occupied at 80 and 20%, respectively. The aggregate composition of the *M*(1) site is $(Nb_{1.91}Sn_{0.05}Ta_{0.03}Ti_{0.01})_{\Sigma 2}$ *apfu*, ideally Nb_2 *apfu*. The [6]-coordinated *M*(2) site is occupied by $(Sc_{0.83}Ta_{0.07}Mn_{0.04}U^{4+}{}_{0.03}W^{6+}{}_{0.02}\ Pb_{0.01})_{\Sigma 1}$ *apfu*, ideally Sc *apfu*. The *M*(3) site splits into two sites, [8]-coordinated Y-dominant *M*(3A) site and [6]-coordinated vacancy-dominant *M*(3B) site, and they are occupied at 78 and 22%. The aggregate composition of the *M*(3) site is $(Y_{0.53}Ln_{0.25}Ca_{0.09}Mn_{0.06}Th_{0.04}U^{4+}{}_{0.03})_{\Sigma 1}$ *apfu*, ideally Y *apfu*. Hence the three *M* sites ideally give $ScYNb_2$ *apfu*.

The M(1) and M(2) octahedra each form a brookite chain along **c** (Pauling & Sturdivant 1928, Sokolova & Hawthorne 2004) (Fig. 5a, b). In the brookite chain, next-nearest-neighbor octahedra are in a staggered configuration, and the resulting kinked chain has a repeat unit of $[Ti_2O_8]^{8-}$ in brookite. In shakhdaraite-(Y), the brookite chains of Nb-dominant M(1A) and Sc-dominant M(2) octahedra have repeat units $[Nb_2O_8]^{6-}$ and $[Sc_2O_8]^{10-}$, respectively. The [8]-coordinated Y-dominant M(3A) polyhedra form a brookite-like kinked chain with a repeat unit $[Y_2O_{12}]^{18-}$ (Fig. 5c). However, each Y-dominant M(3A) polyhedron of one brookite-like chain shares two edges with the two Y-dominant M(3A) polyhedra of the neighbor brookite-like chain (Fig. 5c). Hence M(3A) polyhedra form a layer $[Y_2O_8]^{10-}$. Alternately, the [6]-coordinated vacancy-dominant M(1B) and M(3B) polyhedra each form brookite chains. In the structure of shakhdaraite-(Y), M(1A) and M(2) brookite chains and a layer of [8]-coordinated M(3A) polyhedra alternate along **a** (Fig. 5d).

Where the cation disorder at the two sites in the structure of shakhdaraite-(Y) is not taken into consideration, shakhdaraite-(Y), ideally $ScYNb_2O_8$ ($Z = 2$), is isostructural with samarskite-(Y), ideally $YFe^{3+}Nb_2O_8$ (Britvin *et al*. 2019) (Table 8). Hence shakhdaraite-(Y) is a Sc analogue of samarskite-(Y). Shkadaraite-(Y) can be considered a derivative of the crystal structure of brookite, ideally TiO_2 ($Z = 8$) (Pauling & Sturdivant 1928). Shakhdaraite-(Y) and brookite are related by the substitution $^{[6]}Sc^{3+} + {}^{[8]}Y^{3+} + 2^{[6]}Nb^{5+} \leftrightarrow 4^{[6]}Ti^{4+}$. Substitution of three different larger and heavier cations, Nb^{5+}, Sc^{3+}, and Y^{3+} [$^{[6]}$Nb: $r = 0.64$ Å, $^{[6]}$Sc: $r = 0.745$ Å, $^{[8]}$Y: $r = 1.019$ Å (Shannon 1976)], for Ti ($^{[6]}r = 0.605$ Å) results in lower symmetry, a larger unit-cell volume, and higher density of shakhdaraite-(Y) relative to those of brookite: shakhdaraite-(Y) is monoclinic, space group *P*2/*c*, $V = 292.7$ Å^3, and $D_{calc.} = 5.602$ g/cm^3; brookite is orthorhombic, space group *Pbca*, $V = 256.84$ Å^3, and $D_{calc.} = 4.250$ g/cm^3 (Table 8). In shakhdaraite-(Y), the repeat distance for brookite and brookite-like chains is 5.211 Å (*cf*. 5.138 Å in brookite, Table 8). Shakhdaraite-(Y) is related to heftetjernite, $ScTaO_4$ (Kolitsch *et al*. 2010) (wolframite-type structure) and iwashiroite-(Y), $YTaO_4$ (Hori *et al*. 2006) [fergusonite-(Y)-β structure], as they share similar structural fragments: brookite chains of Sc-octahedra in shakhdaraite-(Y) and heftetjernite and layers composed of brookite-like chains of [8]-coordinated Y-polyhedra in shakhdaraite-(Y) and iwashiroite-(Y).

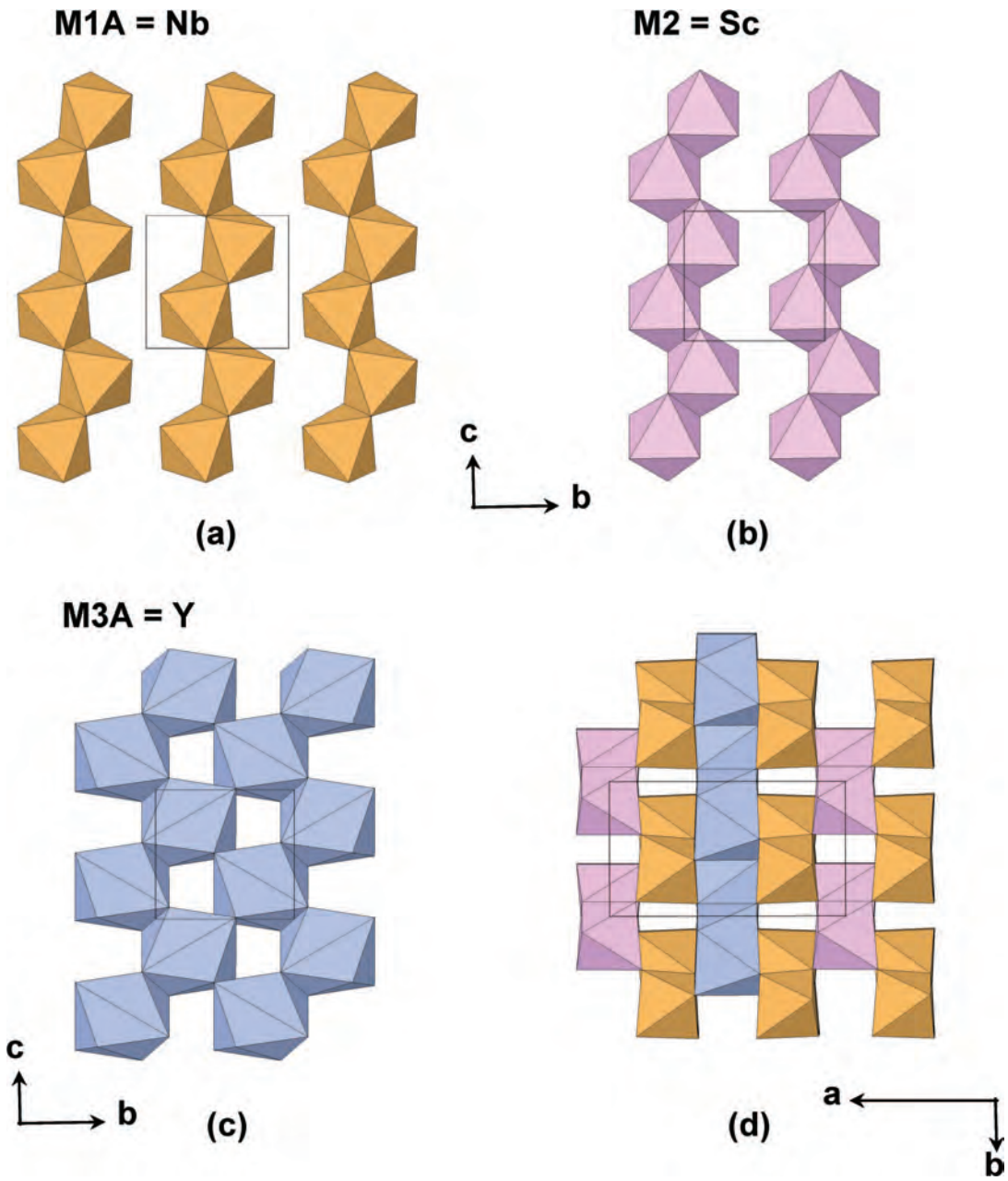

FIG. 5. The crystal structure of shakhdaraite-(Y). (a) The brookite chains of Nb-dominant M(1A) octahedra at $x \sim 0.75$ and (b) Sc-dominant M(2) octahedra at $x = 0$. (c) A layer of the [8]-coordinated Y-dominant M(3A) polyhedra at $x = 0.5$. (d) Alternation of brookite chains of M(1A) and M(2) octahedra and a layer of [8]-coordinated M(3A) polyhedra along **a**. Nb-dominant and Sc-dominant octahedra are orange and pink, respectively; Y-dominant M(3A) polyhedra are blue; vacancy-dominant *M*(1B) and *M*(3B) sites are not shown.

TABLE 8. COMPARISON OF SHAKHDARAITE-(Y), SAMARSKITE-(Y), BROOKITE, IWASHIROITE-(Y), HEFTETJERNITE, AND NIOBOHEFTETJERNITE

Mineral	shakhdaraite-(Y)	samarskite-(Y)[1]	brookite[2]	iwashiroite-(Y)[3]	heftetjernite[4]	niobo-heftetjernite[5]
Ideal formula	$ScYNb_2O_8$	$YFe^{3+}Nb_2O_8$	TiO_2	$YTaO_4$	$ScTaO_4$	$ScNbO_4$
System	monoclinic	monoclinic	orthorhombic	monoclinic	monoclinic	monoclinic
Space group	*P*2/*c*	*P*2/*c*	*Pbca*	*P*2/*a*	*P*2/*c*	*P*2/*c*
a (Å)	9.930(2)	9.8020(8)	9.174(2)	5.262(5)	4.784(1)	4.7092(3)
b	5.663(1)	5.6248(3)	5.449(2)	5.451(5)	5.693(1)	5.6531(4)
c	5.211(1)	5.2073(4)	5.138(2)	5.110(5)	5.120(1)	5.0530(4)
α (°)	90	90	90	90	90	90
β	92.38(3)	93.406(4)	90	95.12(10)	91.15(3)	90.453(3)
γ	90	90	90	90	90	90
V (Å^3)	292.7(5)	286.59(4)	256.84(6)	146.0(2)	139.42(5)	134.515(17)
Z	2	2	8	2	2	2
$D_{calc.}$ (g/cm^3)	5.602	6.210	4.250	7.1	6.44	5.855
Strongest reflections	3.72(35)		3.5091(100)	3.13(100)	4.783(33)	4.722(22)
in the X-ray powder	3.073(100)		3.4618(79)	2.95(94)	3.807(32)	3.776(22)
diffraction data,	2.990(85)		2.8978(95)	2.73(26)	3.662(53)	3.628(44)
d/Å (*I*)	2.604(24)		2.4738(24)	2.62(23)	3.000(100)	2.961(100)
	2.484(33)		1.9670(19)	1.890(29)	2.957(97)	2.938(83)
	1.916(23)		1.8913(29)	1.862(29)	2.4877(34)	2.472(30)

[1] Britvin *et al.* (2019); powder data have not been reported.
[2] Unit-cell parameters and D_{calc} are from the most recent work on brookite (Meagher & Lager 1979). X-ray powder diffraction data are from PDF2 # 76-1934.
[3] Hori *et al.* (2006)
[4] Kolitsch *et al.* (2010)
[5] Lykova *et al.* (2020)

Acknowledgments

We are grateful to Uwe Kolitsch, an anonymous reviewer, and Associate Editor Henrik Friis for their comments which helped to improve the manuscript. We thank T.G. Bakhtibekov, F.K. Rakhimi, P.V. Khvorov, R.U. Sobirova, R.D. Bakhtdavlatov, and I. Oymukhammadzoda for help with the field work and N.N. Koshlyakova for help with the EBSD. This work was supported by a Discovery Grant from the Natural Sciences and Engineering Research Council of Canada to FCH.

References

Astrelina, E., Smirnov, S., Ragozin, A., Karmanov, N., & Konovalenko, S. (2011) Late magmatic crystallization in the tourmaline-bearing miarolitic granitic pegmatites (by example of Shakhdarinskaya and Leskhozovskaya veins, SW Pamir, Tajikistan). ECROFI-XXI, Leoben, Austria, Abstracts, 24–25.

Britvin, S.N., Pekov, I.V., Krzhizhanovskaya, M.G., Agakhanov, A.A., Ternes, B., Schüller, W., & Chukanov, N.V. (2019) Redefinition and crystal chemistry of samarskite-(Y), $YFe^{3+}Nb_2O_8$: Cation-ordered niobate structurally related to layered double tungstates. *Physics and Chemistry of Minerals* **46**, 727–741.

Budanov, V.I. (1993) *Endogenic Formations of Pamir*. Donish, Dushanbe, Tajikistan (in Russian).

Budanova, K.T. & Budanov, V.I. (1983) *Metamorphic Formations of South-Western Pamir*. Donish, Dushanbe, Russia (in Russian).

Černý, P. & Chapman, R. (2001) Exsolution and breakdown of scandian and tungstenian Nb–Ta–Ti–Fe–Mn phases in niobian rutile. *Canadian Mineralogist* **39**, 93–101.

Černý, P., Chapman, R., & Masau, M. (2000) Two-stage exsolution of a titanian $(Sc,Fe^{3+})(Nb,Ta)O_4$ phase in niobian rutile from Southern Norway. *Canadian Mineralogist* **38**, 907–913.

Chupin, V.P., Vladimirov, A.G., Rudnev, S.N., & Osorgin, N.Yu. (1988) Conditions of formation and geochemical features of the high-aluminous granites of the Pamiro-Shugnansky pluton (Southwest Pamir). *In* Thermobarogeochemical Investigations of Processes of Mineral Formation (N.V. Sobolev & I.T. Bak, eds.). Nauka, Novosibirsk, Russia (93–100) (in Russian).

Gagné, O.C. & Hawthorne, F.C. (2020) Bond-length distributions for ions bonded to oxygen: Results for the

transition metals and quantification of the factors underlying polyhedral distortion via bond-length variation. *IUCrJ* **7**, 581–629.

Hori, H., Kobayashi, T., Miyawaki, R., Matsubara, S., Yokoyama, K., & Shimizu, M. (2006) Iwashiroite-(Y), $YTaO_4$, a new mineral from Suishoyama, Kawamata Town, Fukushima Prefecture, Japan. *Journal of Mineralogical and Petrological Sciences* **101**, 170–177.

Kolitsch, U., Kristiansen, R., Raade, G., & Tillmans, E. (2010) Heftetjernite, a new scandium mineral from the Heftetjern pegmatite, Tørdal, Norway. *European Journal of Mineralogy* **22**, 309–316.

Konovalenko, S.I. (2006) Types of the miarolitic pegmatites in the crystalline rocks of Southwest Pamir. *In* Gemmology: Collected Papers. (S.I. Konovalenko, L.A. Zyryanova, O.V. Bukharova, & E.M. Osachakova, eds.). TCSTI, Tomsk (69–75) (in Russian).

Konovalenko, S.I. (2009) Collector's raw materials from the miarolitic pegmatites of the Southwest Pamir. *In* Gemmology: Collected Papers. (S.I. Konovalenko, A.A. Baeva, L.A. Zyryanova, & O.V. Bukharova, eds.). TCSTI, Tomsk (62–75) (in Russian).

Konovalenko, S.I., Sazontova, N.A., & Smirnov, S.Z. (2001) Composition, structure, and formation regime of the miarolitic pegmatites of the Leskhozovskaya vein (Southwest Pamir). Petrology of Magmatic and Metamorphic Complexes Conference, Proceedings **2**, Tomsk, Russia (226–228) (in Russian).

Labuntsov, A.N. (1930) Geological-mineralogical studies at Western Pamir and Badakhshan province in Afghanistan in 1928. Proceedings of the Pamir Expedition **IV**, Mineralogy, 64–66 (in Russian).

Lykova, I., Rowe, R., Poirier, G., McDonald, A.M., & Giester, G. (2020) Nioboheftetjernite, IMA 2019-133. CNMNC Newsletter No. 55. *Mineralogical Magazine* **84**, 485–488.

Meagher, E.P. & Lager, G. (1979) Polyhedral thermal expansion in the TiO_2 polymorphs: Refinement of the crystal structures of rutile and brookite at high temperature. *Canadian Mineralogist* **17**, 77–85.

Pauling, L. & Sturdivant, G.H. (1928) The crystal structure of brookite. *Zeitschrift für Kristallographie* **68**, 239–256.

Peretyazhko, I.S., Prokof'ev, V.Yu., Zagorskiy, V.Yu. & Smirnov, S.Z. (2000) Boric acids in processes of pegmatite and hydrothermal mineral formation: Petrological result of sassolite (H_3BO_3) discovery in fluid inclusions. *Petrologia* **8**, 241–266 (in Russian).

Pouchou, J.L. & Pichoir, F. (1985) 'PAP' φ(ρZ) procedure for improved quantitative microanalysis. *In* Microbeam Analysis (J.T. Armstrong, ed.). San Francisco Press, San Francisco, California, United States (104–106).

Rutte, D., Ratschbacher, L., Khan, J., Stübner, K., Hacker, B.R., Stearns, M.A., Enkelmann, E., Jonckheere, R., Pfänder, J.A., Sperner, B., & Tichomirowa, M. (2017) Building the Pamir Tibetan Plateau – Crustal stacking, extensional collapse, and lateral extrusion in the Central Pamir: 2. Timing and rates. *Tectonics* **36**, 385–419.

Sazontova, N.A., Konovalenko, S.I., & Smirnov, S.Z. (2003) Magmatic crystallization of the two-feldspar-quartz complex of Leskhozovskaya pegmatite (South-Eastern Pamir): Melt and fluid inclusion study. *Acta Mineralogica-Petrographica, Abstract series* **2**, 169–170.

Shannon, R.D. (1976) Revised effective ionic radii and systematic studies of interatomic distances in halides and chalcogenides. *Acta Crystallographica* **A32**, 751–767.

Sheldrick, G.M. (2015) Crystal structure refinement with *SHELX*. *Acta Crystallographica* **C71**, 3–8.

Smirnov, S.Z., Peretyazhko, I.S., Prokof'ev, V.Yu., Zagorskiy, V.Yu. & Shebanin, A.P. (2000) First find of sassolite (H_3BO_3) in fluid inclusions in minerals. *Geologia i geofizika* **41**, 194–206 (in Russian).

Smirnov, S., Sazontova, N., Konovalenko, S.I., Thomas, V.G., Danyushevsky, L., Vladimirova, I.A., & Vladimirov, A.G. (2008) Pegmatite-forming medium at the transition stage from magmatic to hydrothermal crystallization (on example of Leskhozovskaya pegmatite, SW Pamir, Tajikistan). Materials of XIII International conference on thermbarogeochemistry and IV APIRIS symposium. IGEM RAS, Moscow, Russia (153–156) (in Russian).

Sokolova, E. & Hawthorne, F.C. (2004) The crystal chemistry of silicate minerals with chains of (TiO_6) octahedra. *Canadian Mineralogist* **42**, 807–826.

Stearns, M.A., Hacker, B.R., Ratschbacher, L., Rutte, D., & Kylander-Clark, A.R.C. (2015) Titanite petrochronology of the Pamir gneiss domes: Implications for mid-deep crust exhumation and titanite closure to Pb and Zr diffusion. *Tectonics* **34**, 784–802.

Stübner, K., Ratschbacher, L., Weise, C., Chow, J., Hofmann, J., Khan, J., Rutte, D., Sperner, B., Pfänder, J.A., Hacker, B.R., Dunkl, I., Tichomirowa, M., & Stearns, M.A. (2013) The giant Shakhdara migmatitic gneiss dome, Pamir, India-Asia collision zone: 2. Timing of dome formation. *Tectonics* **32**, 1404–1431.

Szełęg, E., Galuskina, I., & Prusik, K. (2010) A Sc-Nb oxide from corundum pegmatites of the Krucze Skały in Karpacz (Karkonosze massif, Lower Silesia, Poland) – A potentially new mineral of the $ScNbO_4$–$FeWO_4$ series. Abstracts, 20th General Meeting of the IMA, Budapest, Hungary, p. 501.

Vinnichenko, G.P., & Kukhtikov, M.M. (1993) The structural position of Pre-Cambrian complexes of South-West Pamir in the system of Mesozoic folded structures in the South-East of Central Asia. *Izvestiya AN Respubliki Tadjikistan. Otdelenie nauk o Zemle (Earth Sciences Department)* **2**, 26–32 (in Russian).

VLADIMIROV, A.G. (2005) Synmetamorphic stress-granites of the Pamir-Himalayas and Central Asia: Comparative characteristic, genesis, and geodynamical conditions of formation. *Proceedings of the All-Russian Conference Petrology of magmatic and metamorphic complexes*, 52–55 (in Russian).

VLADIMIROV, A.G., KRUK, N.N., RUDNEV, S.N., & KHROMYKH, S.V. (2003) Geodynamics and granitoid magmatism of the collision orogens. *Geologia i geofizika* **44**, 1321–1338 (in Russian).

VON KNORRING, O.V. & SAHAMA, TH.G. (1969) Scandian ixiolite from Mozambique and Madagascar. *Bulletin of the Geological Society of Finland* **41**, 75–77.

VÝRAVSKÝ, J., ŠKODA, R., & NOVÁK, M. (2017) Kristiansenite, thortveitite and $ScNbO_4$: Products of Ca-metasomatism of Sc-enriched columbite-(Mn) from NYF pegmatite Koichovice II, Czech Republic. PEG2017, *NGF Abstracts and Proceedings* **2**, 169–172.

WILSON, A.J.C., Ed. (1992) *International Tables for Crystallography*. *Volume C: Mathematical, Physical and Chemical Tables*. Kluwer Academic Publishers, Dordrecht, Netherlands.

Received December 8, 2020. Revised manuscript accepted May 10, 2021.